Universe
Scientific Publishing

Influence of Underflow Diameter on Flow Field Characteristics and Separation Performance of Cyclone Separator

Lihong Wei

School of Intelligent Manufacturing, Leshan Vocational and Technical College, Leshan 614000, China.

Abstract: To explore the impact of varying bottom outlet diameters on the flow characteristics and separation performance of a 70mm primary diameter cyclone separator, we analyze cyclone separators with bottom outlet diameters of 10mm, 12mm, 14mm, and 16mm. The findings reveal that at an inlet velocity of 10m/s and for particle sizes ranging from 10 to 90 μm, cyclone separators with different bottom outlet diameters exhibit consistent trends in tangential velocity, axial velocity, and pressure distribution.As the bottom outlet diameter increases, the split ratio gradually rises, and this effect becomes more pronounced with larger sand particle sizes. The separation efficiency also improves with increasing bottom outlet diameter for a given particle size, and separation efficiency increases for all bottom outlet diameters as particle size grows. The pressure drop decreases as the bottom outlet diameter increases for a given particle size, and the pressure drop diminishes for all bottom outlet diameters with larger particle sizes.Within the scope of this study, it is evident that, for sand particles of the same size, a 16mm bottom outlet diameter yields the highest separation efficiency and the lowest pressure drop, indicating superior separation performance.

Keywords: Cyclone Separator; Underflow Diameter; Split Ratio; Separation Efficiency

1. Introduction

In the process of offshore oil, gas, and hydrate extraction, transporting slurry with a high concentration of sand and sediments can lead to downhole tool blockages and increased energy consumption. Therefore, effective sand removal is of utmost importance. Cyclones, as commonly used separation devices, offer advantages such as ease of operation, simple structure, and high separation efficiency. They are widely applied in industries such as petrochemicals and ore beneficiation [1]. The geometric and operational parameters of cyclones have a significant impact on their separation performance [2], and one critical structural parameter is the underflow diameter, which has been the subject of extensive research.

Liu Peikun et al. [3] conducted a study on the effect of the underflow diameter on cyclone separation granularity and product distribution, finding that a larger underflow diameter leads to a shorter air column formation time. Tian et al. [4] explored the influence of underflow pipe diameter on the performance of hydraulic cyclones, revealing that as the underflow pipe diameter increases, back pressure and axial velocity at the same position inside the underflow pipe also increase. Yin Weiwei et al. [5] analyzed the impact of the underflow spigot diameter on wall wear in cyclones and concluded that the wear rate on the entrance annular space wall remains unchanged with variations in the underflow spigot diameter. Lv Xiuli [6] simulated the internal flow field of cyclones, showing that increasing the underflow spigot diameter results in a decrease in flow velocity within the flow field. Qiu Shunzuo et al. [7] studied the effect of the underflow diameter on cyclone separation performance, indicating that as the underflow spigot diameter increases, separation efficiency initially increases and then decreases, with a significant variation in the magnitude of this change.

However, existing research has primarily focused on different industries and operating conditions, overlooking the influence of cyclone structural parameters on separation performance in the field of hydrate extraction. In the process of offshore oil, gas, and hydrate extraction, the slurry contains water, sand, and hydrates, with the impact of sand on separation efficiency being particularly crucial. Therefore, this paper employs numerical simulation research methods to investigate the impact of different underflow diameters under various particle sizes on the flow characteristics and separation performance of downhole solid-liquid cyclones. This research provides valuable guidance for the design of downhole cyclones in the context of offshore oil, gas, and hydrate extraction.

2. Numerical Simulation

2.1 Geometric Model and Grid Generation

The basic structure of the cyclone separator is illustrated in Figure 1(a). In this study, a cyclone separator with a primary diameter of 70 mm was utilized, with underflow diameters of 10 mm, 12 mm, 14 mm, and 16 mm, while other structural parameters were calculated according to relevant empirical formulas [8]. Specific dimensional parameters are provided in Table 1. Unstructured tetrahedral meshing was carried out using Fluent Meshing software, with particular refinement at key areas, such as the tangential inlet.

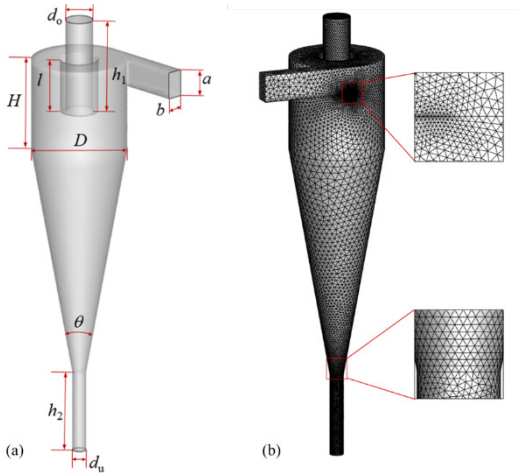

Figure 1 Cyclone Separator Geometry and Grid Division (Underflow Diameter 10 mm)

Table 1 Cyclone Separator Geometric Parameters

Structure	Symbol	Parameter
Main Diameter	D	70mm
Cylindrical Section Length	H	70mm
Overflow Pipe Length	h1	70mm
Overflow Pipe Insertion Depth	l	40mm
Overflow Diameter	d0	20mm
Conical Section Angle	θ	20°
Inlet Dimensions	a×b	20mm×12mm
Underflow Pipe Length	h2	60mm
Underflow Diameter	du	10/12/14/16mm

2.2 Mathematical Model and Boundary Conditions

Given the strong rotational turbulent characteristics and anisotropy within the flow field of cyclones, the Reynolds Stress Model (RSM) is capable of considering cyclone motion and variations in surface curvature along the flow direction. Moreover, many researchers have confirmed that the numerical simulation results using the RSM model closely match experimental results [10,11]. Therefore, this study employs the RSM model as the turbulence model.In the context of multiphase flow modeling, the Mixture model is chosen due to its lower computational demands compared to the Euler model and its excellent stability [12].

The slurry enters the hydraulic cyclone with a vertical inlet velocity of 10 m/s at the inlet section. Steady-state simulations were conducted with a turbulence intensity of 5%. The outlet conditions were set at standard atmospheric pressure, with a solid particle mass fraction of 0. The solid wall boundaries were treated using standard wall functions, assuming a no-slip wall boundary. The pressure-velocity coupling term in the governing equations was solved using a consistent SIMPLE algorithm.For fluid domains with high cyclonic flow and significant

pressure gradients, the pressure difference was resolved using the PRESTO format. Convective terms were discretized using the Second Order Upwind format as well as the QUICK format.

2.3 Physical Properties of the Medium

To consider the impact of underflow diameter on the separation performance of the cyclone separator for different particle diameters, particles with diameters of 10μm, 50μm, and 90μm are taken as the research objects. The physical properties of the mixed slurry are presented in Table 2.

Table 2 Physical Properties of the Mixed Slurry

Medium	Density (kg/m³)	Volume Fraction (%)	Particle Diameter (μm)
Water	1000	95	-
Sand	2600	5	10/50/90

3. Results and Analysis

3.1 Velocity Field

3.1.1 Tangential Velocity

In the process of cyclone separation, the tangential velocity plays a crucial role in determining the magnitude of the centrifugal force and centrifugal acceleration generated by the cyclone, which is of paramount importance for particle separation [13,14]. As shown in Figure 2, along the radial direction from the wall to the center, the tangential velocity first increases and then decreases, forming a characteristic M-shaped peak distribution. This pattern aligns with the typical tangential velocity distribution of a combination vortex. Additionally, the tangential velocity distribution in the cyclone demonstrates excellent axial symmetry, contributing to the stability of the flow field.

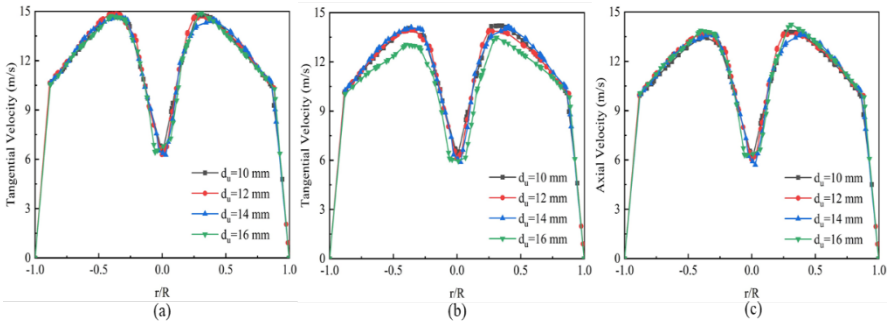

Figure 2 Tangential Velocity Distribution Curves of Cylinder-Cone Junction Surface at Different Underflow Diameters (a: Particle Diameter 10μm; b: Particle Diameter 50μm; c: Particle Diameter 90μm)

3.1.2 Axial Velocity

In cyclone separation, the axial velocity determines the direction of fluid flow. Positive velocity corresponds to a downward flow towards the underflow outlet, while negative velocity corresponds to an overflow towards the overflow outlet. Different axial velocities in various directions contribute to particle separation [15]. As shown in Figure 3, it can be observed that the axial velocity distribution follows a similar pattern for different underflow diameters. Near the wall, there is a positive velocity, while in the center, the axial velocity of the fluid is negative. For the same particle size, as the underflow diameter increases, the velocity of flow in the overflow direction steadily decreases. This facilitates the reduction of sand particles flowing towards the overflow pipe, thus enhancing the separation efficiency.

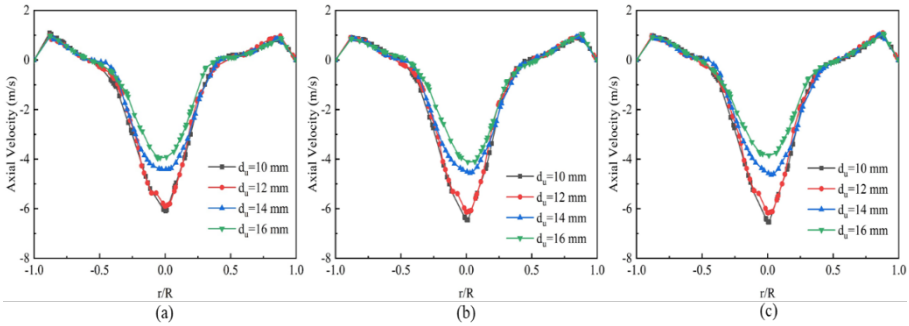

Figure 3 Axial Velocity Distribution Curves of Cylinder-Cone Junction Surface at Different Underflow Diameters

(a: Particle Diameter 10 μm; b: Particle Diameter 50μm; c: Particle Diameter 90μm)

3.2 Pressure Field

The distribution of internal pressure within a cyclone separator significantly impacts the behavior of the medium within the flow field and the separation performance. As seen in Figure 4, the static pressure distribution patterns within cyclone separators with different bottom outlet diameters are generally similar, exhibiting an axisymmetric distribution. Along the radial direction from the wall to the axis, the static pressure gradually decreases, conforming to the static pressure distribution pattern characteristic of a combined vortex flow field.With an increase in sand particle size, the static pressure near the wall gradually decreases, while the difference in static pressure near the axis remains relatively small. Therefore, for larger particle sizes, the energy loss during the separation process is relatively low.

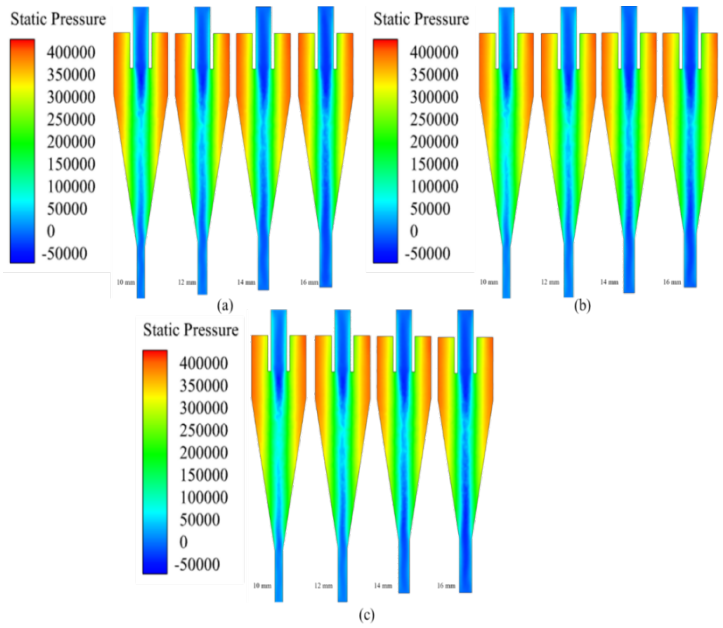

Figure 4 Cloud Maps of Axial Cross-Section Static Pressure Distribution at Different Underflow Diameters

(a: Particle Diameter 10 μm; b: Particle Diameter 50 μm; c: Particle Diameter 90 μm)

3.3 Separation Performance

3.3.1 Split Ratio

From Figure 5, it is evident that, for a given particle diameter, as the underflow diameter increases, the split ratio of the cyclone separator gradually increases. Moreover, this increasing trend becomes more pronounced with larger sand particle diameters. Within the range of sand particle diameters from 10μm to 90μm, the split ratios of the cyclone separator for the four underflow diameters exhibit a basic linear

increase. The split ratio ranges are approximately 0.117 to 0.134, 0.159 to 0.175, 0.226 to 0.247, and 0.308 to 0.374, respectively. Hence, it is apparent that a smaller underflow diameter favors slurry concentration, while a larger underflow diameter facilitates the discharge of more waste materials through the underflow outlet.

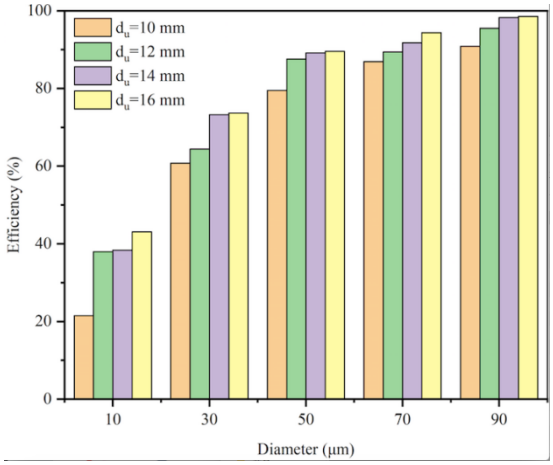

Figure 5 Curve of Separation Efficiency Variation with Sand Particle Diameter at Different Underflow Diameters

3.3.2 Separation Efficiency

From Figure 6, it is evident that, under the same sand particle size, as the underflow diameter increases, the separation efficiency of the cyclone separator also increases. The reason for this is that a smaller underflow outlet diameter limits the sand discharge capacity, leading to the accumulation of some sand particles at the underflow outlet. Ultimately, these particles are carried with the cyclone flow into the overflow pipe, reducing the separation efficiency. However, as the sand particle size increases, the issue of accumulation near the underflow outlet diminishes because larger particles offer greater resistance to the inward spiraling flow and find it challenging to enter the overflow pipe. Consequently, within the range of sand particle sizes between 10 and 90 μm, the separation efficiency continues to improve.In this study, the influence of sand particle size on separation efficiency exhibits a consistent trend under different underflow outlet diameters. For instance, with a 10 mm underflow outlet, the separation efficiency for 10 μm particle size is only 21.5%, while the separation efficiency for 90 μm particle size reaches 90.8%.

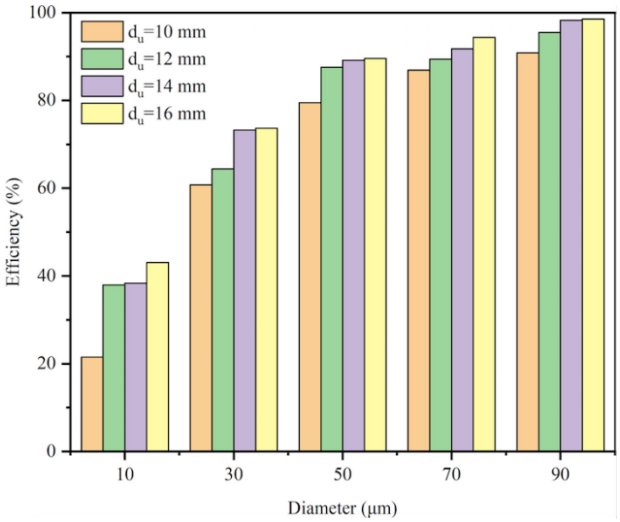

Figure 6 Curve of Separation Efficiency Variation with Sand Particle Diameter at Different Underflow Diameters

3.3.3 Pressure Drop

From Figure 7, it is evident that, with increasing sand particle diameter, the pressure drop of the cyclone separator exhibits a similar decreasing trend for the four underflow diameters. For a given sand particle diameter, the cyclone separator with a 16mm underflow diameter

experiences the smallest pressure drop, implying the lowest pressure loss at this point. This phenomenon is attributed to the larger underflow diameter leading to a reduced exit velocity of the underflow fluid, thereby diminishing the turbulent intensity in the conical section of the cyclone separator and subsequently lowering the overall energy losses.

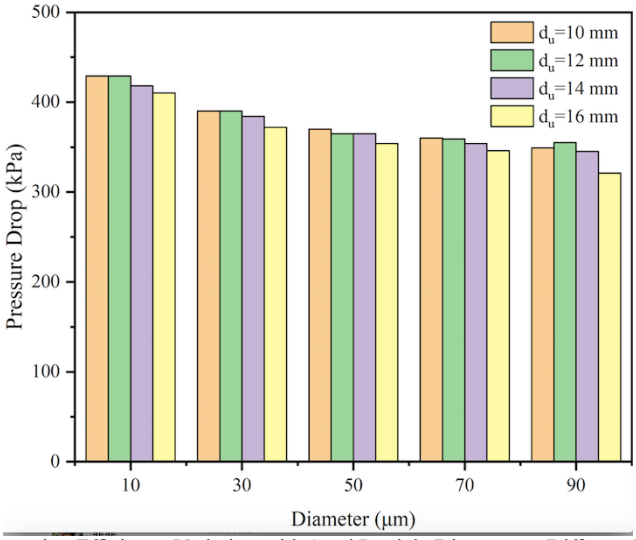

Figure 7 Curve of Separation Efficiency Variation with Sand Particle Diameter at Different Underflow Diameters

Conclusion

(1) For the same particle size, changes in the underflow diameter have a minimal impact on the tangential velocity of the cyclone. As the underflow diameter increases, the fluid's velocity in the direction of overflow steadily decreases. This is advantageous in reducing the flow of sand particles into the overflow pipe, thereby enhancing separation efficiency.

(2) Cyclones with different underflow diameters exhibit similar static pressure distribution patterns. With an increase in sand particle size, the static pressure near the cyclone wall gradually decreases, while the static pressure near the cyclone axis remains relatively consistent. Consequently, energy losses progressively diminish.

(3) The split ratio increases with the enlargement of the underflow diameter, and this trend becomes more pronounced with larger sand particle sizes. Under the same particle size, the separation efficiency of cyclones improves as the underflow diameter increases, and the separation efficiency of cyclones with various underflow diameters also increases with larger particle sizes. Furthermore, under the same particle size, the pressure drop in cyclones decreases as the underflow diameter increases, and the pressure drop of cyclones with different underflow diameters also decreases with larger particle sizes.

(4) Within the scope of this study, it was observed that, for sand particles of the same size, the hydrocyclone achieved its highest separation efficiency and lowest pressure drop when the bottom flow diameter was set at 16mm, thus demonstrating its optimal cyclonic separation performance.

References

[1] Xiao X. Current Status and Development Trends of Hydraulic Cyclone Applications[J]. Chemical Equipment and Piping, 2018, 55(03): 37-41.

[2] Wu YX, Xu JY. Current Status and Development Trends of Oil-Water Separation Technology[J]. Advances in Mechanics, 2015, 45(45).

[3] Zhang YK, Yang M, Liu PK, et al. Influence of Structural Parameters on the Performance of Air Column in Double Overflow Hydrocyclone[J]. China Mining Magazine, 2019, 28(09): 169-174.

[4] Tian JY, Ni L, Song T, et al. Numerical Study of Foulant-Water Separation Using Hydrocyclones Enhanced by Reflux Device: Effect of Underflow Pipe Diameter[J]. Separation and Purification Technology, 2019, 215: 10-24.

[5] Yin WW, Fan FS, Yuan HX, et al. Influence of Underflow Outlet Diameter on Wall Erosion in Solid-Liquid Separation Hydrocyclone[J]. Food Industry, 2017, 38(11): 228-232.

[6] Lv XL. Study on the Influence of Hydrocyclone Underflow Outlet Diameter and Feed Properties on Solid Particle Motion[J]. Coal Preparation Technology, 2017(05): 5-8.

[7] Qiu SZ, Wang GR Zhou SW, et al. Structural Design and Optimization of In-Situ Purification Separator for Subsea Natural Gas Hydrates[J]. China Offshore Oil and Gas, 2019, 31(02): 125-131.

[8] Pang XS. Theory and Application of Hydraulic Cyclone[M]. Changsha: Central South University Press, 2005.

[9] Zhou S. Numerical Simulation and Model Study on Discharge State of Hydrocyclone Underflow[J]. Wuhan University of Science and Technology, 2020.

[10] Bhaskar KU, Murthy YR, Raju MR, et al. CFD Simulation and Experimental Validation Studies on Hydrocyclone[J]. Minerals Engineering, 2006, 20(1).

[11] Narasimha, Brennan, Holtham. A Review of CFD Modelling for Performance Predictions of Hydrocyclone[J]. Engineering Applications of Computational Fluid Mechanics, 2007, 1(2).

[12] Wang DF, Wang GR, Qiu SZ, et al. Influence of Overflow Pipe Structure on Separation Performance of Gas Hydrate Hydrocyclone[J]. Journal of Process Engineering, 2019, 19(05): 982-988.

[13] Zhao QG, Zhang MX. Hydrocyclone Separation Technology[M]. Chemical Industry Press, 2003.

[14] Ai XM, Hua WX, Zhang QX, et al. Simulation Study on Single-Phase Flow Characteristics of Oil-Water Hydrocyclone Based on RSM Model[J]. Petroleum Drilling Techniques, 2020, 49(02): 27-31.

[15] Huang Y. Research and Application of High-Speed Rotation of Particles in Cyclone Field[D]. East China University of Science and Technology, 2017.

[16] Kelsall DF. A Further Study of the Hydraulic Cyclone[J]. Chemical Engineering Science, 1953, 2(6): 254-272.

[17] Wang DF, Wang GR, Zhong L, et al. Effects of Inlet Quantity on Flow Field Characteristics and Separation Performance of Natural Gas Hydrate Slurry in Cyclonic Separator[J]. Shipbuilding of China, 2019, 60(04): 161-169.

[18] Tian JY. Study on Enhancement of Sewage Cyclone Separation Patterns by Injection [D]. Harbin Institute of Technology, 2019.